

Creep Properties of Austenitic Stainless-Steel Weld Metals

A. Nassour, W.W. Bose, and D. Spinelli

(Submitted 27 June 2001)

The creep behavior of two austenitic stainless-steel weld metals was investigated. Two AISI 316L stainless-steel base plates were welded together using the submerged arc-welding process. Creep tests were carried out on the welds at constant load, over a stress range of 100 to 400 MPa, and in the temperature range of 600 to 700 °C. The relationships between stress and minimum secondary creep rate at a constant temperature were obtained with Norton's law. The results showed that AISI 347 weld metal presented a higher creep resistance with lower values of the minimum strain rate, and, consequently, it exhibited a longer life before rupture than AISI 316L weld metal. However, this weld metal showed a lower ductility value than AISI 316L weld metal. The weld-metal microstructure survey, performed before and after the creep testing, has shown different amounts of delta ferrite, which was strongly dependent on time, temperature, and stress level.

Keywords austenitic stainless steel, creep properties, weld metal

1. Introduction

Austenitic stainless steels have been widely used by chemical, petrochemical, power, and nuclear industries for fabrication of many engineering components. In such installations, welded joints are frequently the sites of microstructural heterogeneities, as well as material discontinuities. The association of these regions with some geometric factors that would cause stress concentration may result in a lower level of creep ductility.^[1–3]

The major problem in welding austenitic stainless steel is its susceptibility to develop hot cracking during the welding process. To avoid this problem, small amounts of alloying elements, which stabilize the delta ferrite phase, are normally added to the weld bead through the electrodes. Generally, 3 to 9% of delta ferrite is specified as the necessary amount to avoid crack formation during welding. However, due to the brittle nature of the sigma phase, an upper level of delta ferrite has to be considered, since, when delta ferrite is kept for a long time at elevated temperature, it may transform to sigma phase with the additional formation of chromium carbides.

Many components of energy generator systems are subjected to severe operational conditions, such as high temperature and pressure, which may cause creep failure. Under these conditions, severe degradation of such components may occur as a combination of several factors, such as long service exposure, high-temperature environment, loading conditions, and phase transformations. Failure in most of these cases has been the result of crack propagation that may nucleate at inclusions, second phases, or defects from any fabrication process.^[4]

Despite the wide use of austenitic stainless-steel weld metals,

very little data have been made available concerning the high-temperature creep properties, for example, the AISI-316L stainless steel used frequently in power plant projects.^[5] The construction of these plants involves different welding processes and components from different sections. Studies evaluating the parent-material creep property have already been presented.^[6] However, little information is available concerning the stainless-steel, weld-metal creep mechanical properties.

Gooch^[7] has shown that some weldments may undergo modification in the microstructure composition if loaded for a long time at high temperatures, which, in turn, may lead to changes in the weld-metal mechanical properties. Therefore, the evaluation of mechanical properties at high temperature is very important since it may help to define the component's useful life.

The aim of this study was the evaluation and analysis of some parameters representing the creep properties of two stainless-steel weld metals.

2. Experimental Procedures

The weld metals were produced by the submerged arc welding process, using an AISI 316L steel parent plate and two commercial stainless-steel consumable electrodes, AWS ER316L and AWS ER347. Each weld consisted of only one pass, which was deposited without parent-plate preheating and using a heat input of 3.2 kJ/mm. Therefore, two stainless-steel weld metals were obtained with two different chemical compositions, and they were denoted, according to the consumable electrode, as weld metals 316L and 347. The weldments were not heat treated.

Specimens were removed longitudinally to the welding direction. Tensile tests were carried out at 25, 500, 600, and 700 °C, following the ASTM E21-79 and ASTM E8M-90a standards.^[8,9]

The creep rupture testing followed the ASTM E139-83^[10] recommendation and was carried out at constant-load applied stresses in the ranges of 180 to 400 MPa, 150 to 300 MPa, and 100 to 250 MPa at 600, 650, and 700 °C, respectively.

A. Nassour, W.W. Bose, and D. Spinelli, SMM, Escola de Engenharia de São Carlos, USP Avenida Trabalhador São-Carlense, 400. CEP 13566-590 - São Carlos - SP - Brasil. Contact e-mail: waldek@sc.usp.br.

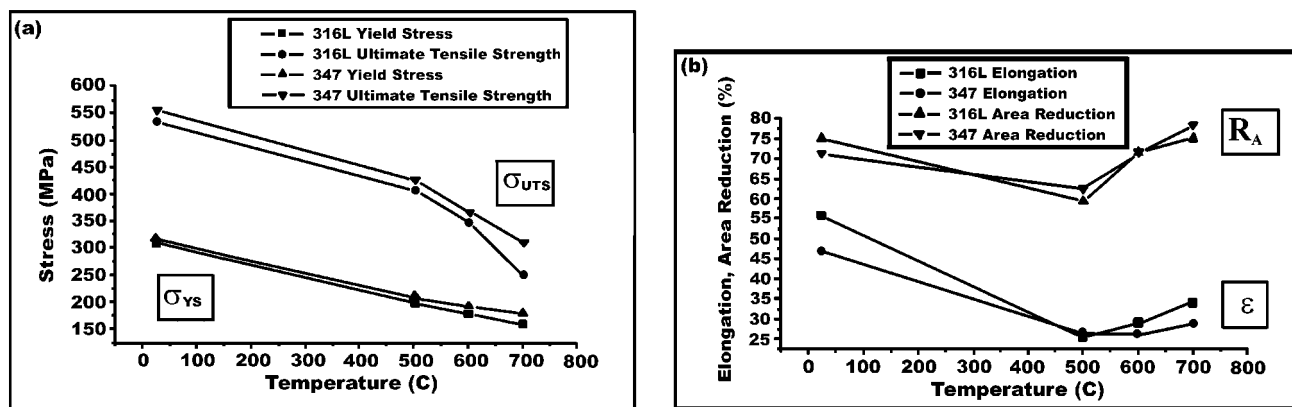


Fig. 1 Weld metal tensile properties: (a) yield and ultimate tensile strength and (b) elongation and area reduction

Table 1 Chemical composition, wt.%

Materials	Alloying element (wt.%)									
	Cr	Ni	Mo	C	Si	Mn	Nb	P	S	N
Parent plate	17.84	10.62	2.04	0.031	0.55	1.63	...	0.026	0.007	0.054
Electrode										
AWS ER-316L	19.00	12.42	2.68	0.016	0.40	1.66	...	0.014	0.014	...
AWS ER-347	19.60	9.65	0.06	0.048	0.42	1.38	0.67	0.020	0.010	...
Weld metal										
316L	18.30	11.90	2.32	0.026	0.60	1.53	...	0.019	0.007	0.058
347	18.50	10.50	1.15	0.035	0.58	1.38	0.30	0.008	0.009	0.061

Temperature control was with a Chromel-Alumel (Villares S.A., Brazil) thermocouple attached directly to the center of the specimen. Both the grips and the extensometers arms were made from superalloy NIMONIC-80A (Electrometal-Special Alloys, Brazil). The system allowed strain rate measurements as low as 10^{-5} h^{-1} .

3. Results

The chemical compositions of the stainless-steel base material, electrodes, and weld metals are given in Table 1.

The 0.2% yield strength, $\sigma_{0.2\%}$, ultimate tensile strength, σ_{UTS} , total elongation at rupture, EL , and reduction of area, RA , obtained at temperatures of 25, 500, 600, and 700 °C, are presented in Fig. 1.

The minimum creep strain rate in the secondary stage, ϵ_s , total creep strain in rupture, ϵ_r , reduction of area, RA , and rupture time, t_r , are shown in Table 2, as well as the amount of delta ferrite before and after the creep test. The applied stress and minimum strain rate in the second stage correspond to the nominal values obtained using the initial specimen size.

4. Discussion

4.1 Tensile Tests

From the results presented in Fig. 1, it is possible to notice that, in the temperature range of 500 to 700 °C, weld metal

347 exhibited a superior mechanical strength to weld 316L, and it became more noticeable as the test temperature increased. This was attributed to a higher carbon content and the niobium addition (which caused the matrix strengthening). It may also be due to a slightly higher amount of delta-ferrite found in weld metal 347 (Table 2). Measurements of ferrite content were made using a Magne-Gage (Fisher, Brazil) calibrated with standards according to AWS Standard A4.2-74.^[11] The effect of the amount of delta ferrite transformed was discussed in detail by Nassour.^[12]

The niobium addition in austenitic steels is normally performed to reduce the susceptibility to intergranular corrosion caused by precipitation of chromium carbides ($M_{23}C_6$).^[13] Niobium carbides (NbC) are more stable and do not dissolve until the temperature reaches approximately 1300 °C. Therefore, the addition of niobium avoids the sensitization phenomenon during the weld-metal cooling cycle, mainly in the temperature range of 590 to 820 °C, which is the temperature range of maximum kinetics formation of chromium carbides, such as $M_{23}C_6$.^[14] In weld metal 347, the strengthening effect due to niobium addition is similar to the one reported in previous studies of the alloying effect on austenitic stainless steels.^[14,15]

4.2 Creep Properties

The creep curves analysis has shown that both weld metals presented the expected behavior when tested in the temperature range studied here (for example, Fig. 2). They exhibited well-defined primary, secondary, and tertiary creep regions. As can be seen in this figure, the creep curves obtained at 600 °C show

Table 2 Creep rupture properties of weld metals

Weld metals	T (°C)	σ_{app} (MPa)	$\epsilon_s \times 10^{-5}$ (h ⁻¹)	ϵ_r (%)	RA (%)	t_r (h)	Delta ferrite (%)	
							Before	After
316L	600	180	3.9	30.1	52.3	3447	5.1	<0.1
		200	20.1	41.9	55.4	1216
		250	250	45.7	67.4	60.2
		300	741	43.6	53.5	29.2	5.2	3.8
		350
	650	150	63.6	44.3	66.4	387	6.3	<0.1
		175	321	40.7	66.9	65.8
		200	831	41.6	69.5	27.7
		250	11,111	41.6	73.4	2.1	6.0	3.2
		300
	700	100	52.9	61.7	74.0	536	4.8	<0.1
		125	176.1	54.8	73.2	159
		150	1,255	52.0	70.8	23.7
		200	24,389	56.0	75.0	1.4	6.2	0.7
		250	0.9	11.2	12.6	2534	6.6	1.7
347	600	300	1.9	14.3	30.6	831
		350	6.5	19.7	35.1	262
		400	196.7	22.7	40.4	9.6	5.0	3.7
		450
		500
	650	200	0.7	18.4	28.3	333	6.7	0.9
		250	7.9	16.3	26.0	152
		275	11.4	13.0	23.0	98.6
		300	39.8	15.3	25.3	65.9	4.1	2.1
		350
	700	175	9.7	12.9	28.3	313	5.5	0.4
		200	35.5	13.6	20.6	44.3
		250	235	22.8	31.3	8.6	5.6	1.3
		300
		350

Table 3 Stress exponent *n* and constant *A* for 316L and 347 weld metals

Weld metals	T (°C)	Applied stress (MPa)	$\epsilon_s = A(\sigma)^n$		
			<i>n</i>	<i>A</i>	<i>R(a)</i>
Type 316L	600	180–300	10.28	3.47×10^{-28}	0.9720
	650	150–250	9.95	1.38×10^{-25}	0.9933
	700	100–200	9.05	2.93×10^{-22}	0.9811
Type 347	600	250 and 300	4.20	7.46×10^{-16}	1.0
	600	300–400	15.94	4.33×10^{-45}	0.9096
	600	250–400	10.8(b)	$5.81 \times 10^{-32}(b)$	0.8423(b)
	650	200–300	9.57	7.03×10^{-28}	0.9810
	700	175–250	8.88	1.26×10^{-24}	0.9987

(a) *R* = correlation coefficient

(b) Values of *n*, *A*, and *r*, if two different steps are not considered

a short primary stage with the majority of plastic deformation occurring inside of the secondary and tertiary creep stages.

The primary and secondary creep stages are strongly affected by the material susceptibility to strain hardening and by the thermally activated dislocation recovery process. In the primary stage, the strain-hardening effect, due to dislocation formation, commands the deformation process, while the balance between strain hardening and recovery of the structure characterizes the secondary stage. In the third region, the increase in the creep rate is generally attributed to the occurrence of one or more effects, such as mechanical instability due to necking, development of internal creep damage, or microstructural instability. Generally, in weld metals, many subgrain structures are formed during the rapid weld solidification; this is due to the accommodation process of the adjacent delta-ferrite dendrites. Therefore, in most weld metals, depending on test conditions, a short or absent primary stage and large secondary and tertiary creep stages are expected.^[3,14]

A progressive reduction in the rupture time with increasing temperature and applied stress was observed. When both weld metals are compared, it is possible to find two very distinct ductility levels, as shown in Fig. 3. For the same temperature and applied stress condition, weld metal 316L always exhibited superior ductility values. For weld metal 316L, at rupture, a temperature of 600 °C, and an applied stress of 250 MPa, values of $\epsilon_r = 45\%$, $RA = 67\%$, and $t_r = 60.2$ h were found. At the same testing condition for weld metal 347, the following values were obtained: $\epsilon_r = 11\%$, $RA = 12\%$, and $t_r = 2534$ h. Comparing these results, it is possible to see that weld metal 347 exhibited ϵ_r and RA values 75 and 86%, respectively, lower than the values found for weld 316L. However, weld metal 347, with niobium and molybdenum additions, has presented an increase of 4200% in rupture time, proving it to be much more resistant to the creep phenomena than weld metal 316L. In weld metal 347, niobium forms carbides or carbonitrides, which cause strengthening by acting as barriers to the movement

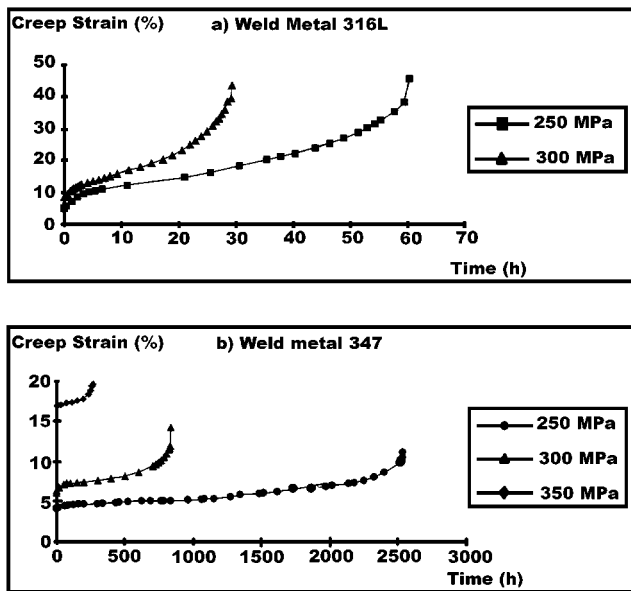


Fig. 2 Typical creep curves for (a) 316L and (b) 347 stainless-steel weld metals tested at 600 °C

of dislocations, leading to lower values of the creep strain rate. According to Folkhard,^[14] Harding and Honeycombe,^[15] and Shinoda *et al.*,^[16] in the temperature range of 600 to 800 °C, there is the formation of niobium carbides and the sigma phase is relatively fast, which contributes even more to the strengthening of the matrix. The weld-metal microstructure survey performed before and after the creep testing has shown different amounts of delta ferrite, which is seen to be strongly dependent of time, temperature, and stress level (Table 2).

It is well established that the creep rate is dependent on material and applied stress, and there is considerable evidence that, under most circumstances, in the secondary creep stage, the creep rate is a power-law function of the applied stress. The creep power law (Norton's law) can be represented by the equation

$$\epsilon_s = A(\sigma)^n \quad (\text{Eq 1})$$

where ϵ_s is the creep strain rate, σ is the applied stress, and A and n are material constants for each temperature.^[17,18]

Figure 4 shows, for the secondary stage, the correlation between the logarithm of the minimum creep rate and the logarithm of the applied stress. It can be seen that there is good agreement between the experimental results and the curve fitted using the Norton's power-law function for all but one case. Using linear regression, the values of the stress exponent, n , and the constant, A , for each temperature were obtained. The results are summarized in Table 3, and the functions that describe the dependence of the minimum creep rate with applied stress for weld metal 316L at different temperatures are defined by the following equations:

$$\epsilon_s = 3.47 \times 10^{-28}(\sigma)^{10.28} \quad \text{at } 600 \text{ }^\circ\text{C} \quad (\text{Eq 2})$$

$$\epsilon_s = 1.38 \times 10^{-25}(\sigma)^{9.95} \quad \text{at } 650 \text{ }^\circ\text{C} \quad (\text{Eq 3})$$

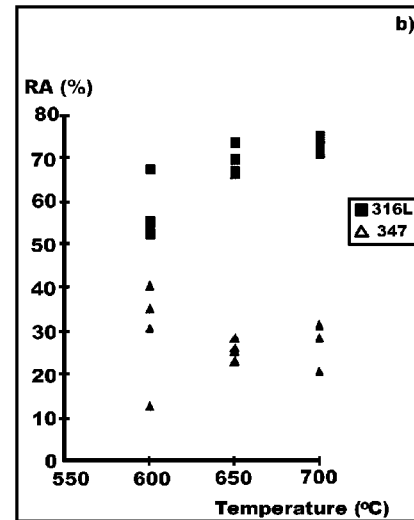
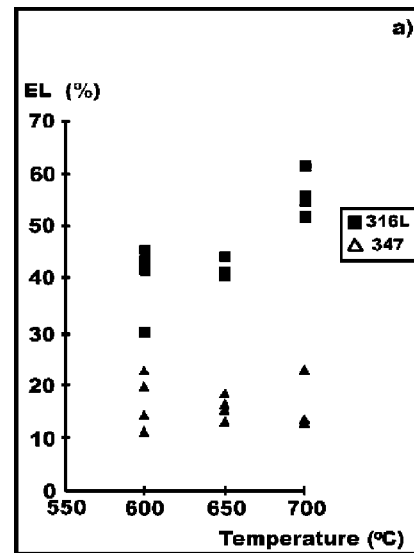


Fig. 3 (a) and (b) Creep ductility properties of 316L and 347 weld metals

$$\epsilon_s = 2.93 \times 10^{-22}(\sigma)^{9.05} \quad \text{at } 700 \text{ }^\circ\text{C} \quad (\text{Eq 4})$$

and for weld metal 347:

$$\epsilon_s = 5.81 \times 10^{-32}(\sigma)^{10.8} \quad \text{at } 600 \text{ }^\circ\text{C} \quad (\text{Eq 5})$$

$$\epsilon_s = 7.03 \times 10^{-28}(\sigma)^{9.57} \quad \text{at } 650 \text{ }^\circ\text{C} \quad (\text{Eq 6})$$

$$\epsilon_s = 1.26 \times 10^{-24}(\sigma)^{8.88} \quad \text{at } 700 \text{ }^\circ\text{C} \quad (\text{Eq 7})$$

The n value is directly related to the mechanism responsible for the creep deformation process, and it varies depending on material. Brown and Ashby,^[19] analyzing data from many different materials, observed that constant A values may range from less than 1 to 10^{15} and that there is also a correlation between the values of n and A , that is, as n increases A also increases. From the results presented in Table 3 and Fig. 5, a

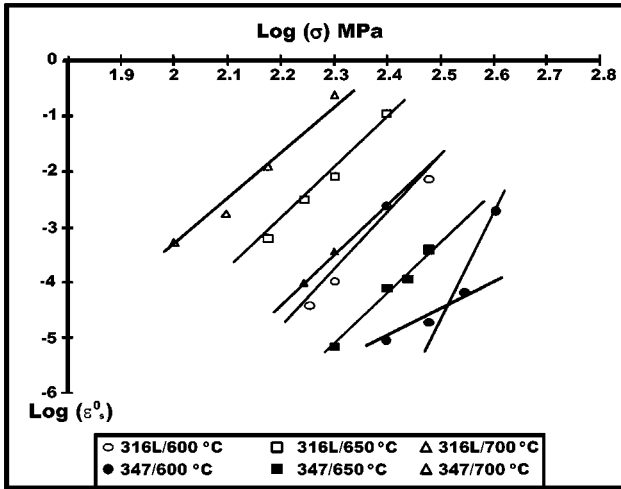


Fig. 4 Minimum creep rate vs initial applied stress

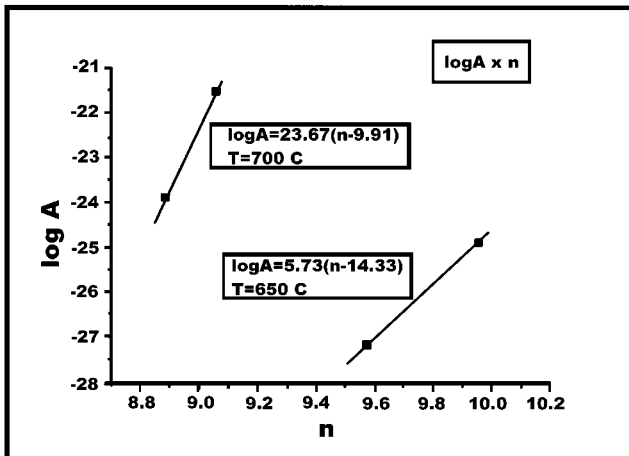


Fig. 5 Correlation between A and n

similar trend is observed between n and A at the same temperature; however, there is also the influence of the testing temperature. At 650 °C, the correlation was

$$\log(A) = 5.73(n - 14.33) \quad (\text{Eq 8})$$

and at 700 °C:

$$\log(A) = 23.67(n - 9.91) \quad (\text{Eq 9})$$

With increasing temperature, the value of $\log(A)$ increases, while the value of n decreases (Fig. 6). Considering the temperature range studied here, the dependence on temperature may be taken as linear and be given by

$$\log(A) = 0.05T - 58.02 \quad (\text{Eq 10})$$

$$n = -0.14T + 18.8 \quad (\text{Eq 11})$$

Comparing the results between weld metals 316L and 347

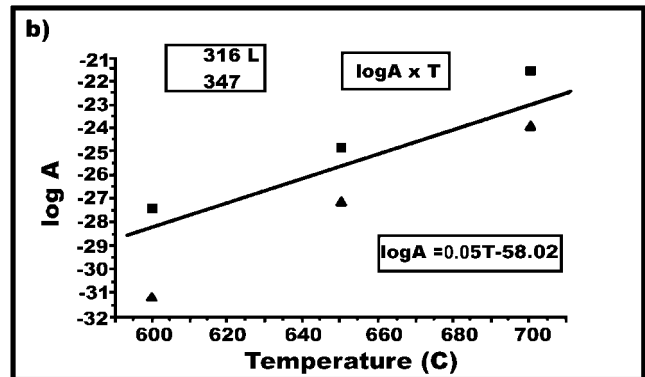
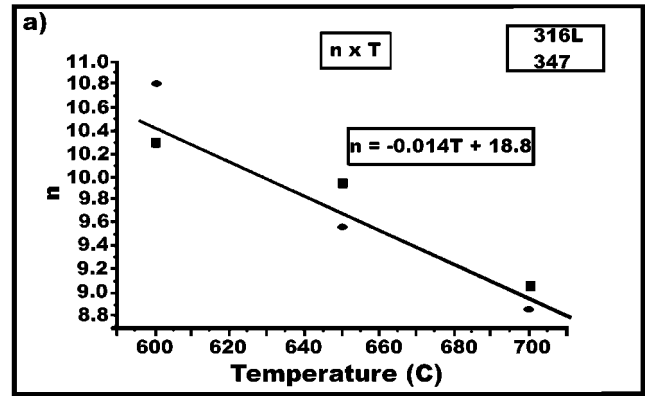


Fig. 6 (a) n and (b) $\log(A)$ dependence on temperature

(Table 3 and Eq 2 through 7), it is possible to notice that for each temperature the values of n for both weld metals are quite similar, while the A values present a great discrepancy. This discrepancy may be responsible for the poor correlation coefficient (0.8) found for Eq 10.

It is also seen that at 600 °C, weld metal 347 presents a lower r value, showing that the result may not be represented by a single equation. Therefore, in this case, it is necessary to consider a two-step regression, one equation for low strain rates and another for high strain rates, and Eq 5 becomes

$$\epsilon_S = 7.46 \times 10^{-16}(\sigma)^{4.2} \text{ at } 600 \text{ }^\circ\text{C}, \text{ for } \sigma \leq 300 \quad (\text{Eq 12})$$

$$\epsilon_S = 4.33 \times 10^{-45}(\sigma)^{15.94} \text{ at } 600 \text{ }^\circ\text{C}, \text{ for } 300 \leq \sigma \leq 400 \quad (\text{Eq 13})$$

This behavior may be caused by a change in the creep micromechanism as the stress increases. At lower stresses, the deformation may be controlled by a grain-boundary sliding or diffusional creep mechanism, and at high stresses, it changes to a dislocation controlled-creep mechanism.^[20] Morris and Harries^[20] have investigated the AISI-316 stainless-steel creep behavior and observed that the values of the stress exponent, n , vary between 3 and 22 for the interval of temperature from 525 to 900 °C with the applied stress range of 20 and 500 MPa. Morris and Harries found $n = 4.2$, and it is higher than that expected for the diffusional creep mechanism ($n = 1$). This

was considered to be a consequence of the test being carried out in the transition region between dislocation and diffusion creep, where the intermediate stress exponent, n , may be expected.

For similar temperature and applied stress, the results showed that weld metal 347 exhibited lower values of minimum creep rates in the secondary stage, indicating higher rupture strength. The n and A values shown in Table 3 are in good agreement with the creep mechanism required to activate the breakage of the dislocation rings, and its subsequent slipping (Orowan mechanism), associated with the climbing movement of dislocations, as suggested by Morris and Harries,^[20] Lagnborg,^[21] and Frost and Ashby.^[22] Thus, the temperature and stress dependence of the creep rate in 316L and 347 weld metals are consistent with the hypothesis that the creep rate is determined by the stress-assisted, thermally activated breakage of the dislocations link and by the subsequent glide of the mobile dislocation link.

5. Conclusions

- The 347 stainless-steel weld metal shows higher rupture time values when compared to the 316 stainless-steel weld metal in similar creep testing conditions due to the strengthening effect of the niobium.
- Two levels of ductility were obtained from the creep testing. Weld metal 316L exhibited a higher level of ductility than the 347 weld metal. This was due to the formation of niobium carbides or carbonitrides, which act as barriers to the movement of dislocations, leading to lower values of creep strain rate in weld metal 347. Consequently, weld metal 347 presented a higher creep resistance.
- The weld-metal microstructure survey, performed before and after creep testing, has shown different amounts of delta ferrite, which has been seen to be strongly dependent on time, temperature, and stress level.
- The values for the stress exponent, n , and constant, A , obtained for the two austenitic weld metals investigated

here, are similar to the values found for austenitic stainless steels. Therefore, the same creep mechanism found for austenitic stainless steel was assumed for the present weldments.

References

1. *Metals Handbook*, 9th ed., ASM, Materials Park, OH, 1980, vol. 3, p. 3.
2. S. Polgary: *Proc. Conf. on Stainless Steels '84*, Göteborg, 1984, Institute of Metals, London, 1985, p. 286.
3. J.J. Smith and R.A. Farrar: *Int. Mater. Rev.*, 1993, vol. 38 (1), p. 25.
4. P.K. Liaw, A. Saxena, and J. Schaefer: *J. Miner. Met. Mater. Soc.*, 1992, vol. 44 (2), p. 43.
5. R.G. Thomas, R.D. Nicholson, and R.A.R. Farrar: *Met. Technol.*, 1984, vol. 11 (2), p. 61.
6. M.D. Mathew, G. Sasikala, S.L. Mannan, and P. Rodriguez: *J. Eng. Mater. Technol.*, 1993, vol. 115 (2), p. 163.
7. T.G. Gooch: *Proc. Conf. on Stainless Steels '84*, Göteborg, 1984, Institute of Metals, London, 1985, p. 249.
8. ASTM E21-79 (reapproved 1988), ASTM, Philadelphia, PA, 1991, vol. 03.01, p. 190.
9. ASTM E8M-90a, ASTM, Philadelphia, PA, 1991, vol. 03.01, p. 146.
10. ASTM E139-83 (reapproved 1990), ASTM, Philadelphia, PA, 1991, vol. 03.01, p. 309.
11. AWS A4.2-74 (reapproved 1975), AWS, Miami, FL, 1975, pp. 1-16.
12. A.C. Nassour: Ph.D. Thesis, Universidade de São Paulo, São Paulo, Brazil, 1995.
13. R.A. Lula and I.M. Bernstein: *Handbook of Stainless Steels*, McGraw-Hill, New York, NY, 1977, p. 1.
14. E. Folkhard: *Welding Metallurgy of Stainless Steels*, Springer-Verlag, New York, NY, 1988.
15. H.J. Harding and R.W.K. Honeycombe: *J. Iron Steel Inst.*, 1966, vol. 20, p. 259.
16. T. Shinoda, T. Ishii, R. Tanaka, T. Mimino, K. Kinoshit, and I. Minegishi: *Metall. Trans.*, 1973, vol. 4, p. 1213.
17. P. Greenfield: *Creep of Metals at High Temperatures*, Mills & Boon, London, 1972.
18. G. Bernasconi and G. Piatti: *Creep of Engineering Material and Structure*, Applied Science, London, 1978.
19. A.M. Brown and M.F. Ashby: *Scripta Metall.*, 1980, vol. 14 (12), p. 1297.
20. D.G. Morris and D.R. Harries: *Met. Sci.*, 1978, vol. 12 (11), p. 525.
21. R. Lagnborg: *Int. Rev.*, 1972, vol. 17 (2), p. 130.
22. H.J. Frost and M.F. Ashby: *Deformation Mechanics Maps*, Pergamon Press, Oxford, United Kingdom, 1982, p. 62.